PHYSICAL REVIEW E VOLUME 53, NUMBER 6 JUNE 1996

Nonlinear dielectric relaxation spectroscopy of the antiferroelectric liquid crystal 4-(1-trifluoromethyl-pheptyloxycarbonyl) phenyl 4′-octyloxybiphenyl-4-carboxylate

Yasuyuki Kimura and Reinosuke Hayakawa
Department of Applied Physics, Faculty of Engineering, The University of Tokyo, Hongo 7-3-1, Bunkyo-ku, Tokyo 113, Japan

Nobuhiro Okabe and Yoshiichi Suzuki
Central Research and Development Laboratory, Showa Shell Sekiyu Kabushiki Kisha, 123-1 Shimokawairi, Atsugi, Kanagawa 243-02, Japan

(Received 31 January 1996)

The linear and third-order nonlinear dielectric constants of the antiferroelectric liquid crystal 4-(1-trifluoromethyl-pheptyloxycarbonyl) phenyl 4′-octyloxybiphenyl-4-carboxylate were experimentally studied in its smectic-*A* (Sm-*A*) and smectic-C_A^* (Sm-C_A^*) phases. Both dielectric constants showed a critical behavior near the Sm-*A*–Sm-C_A^* phase transition corresponding to the softening of ferroelectric soft mode and the increase of the fluctuation in the tilt direction. In the Sm-C_A^* phase, no relaxation was observed in the linear spectrum, but the third-order nonlinear dielectric spectrum showed a Debye-type relaxation with a relaxation frequency of a few kHz corresponding to the Goldstone mode in the Sm-C_A^* phase. This nonlinear response was theoretically analyzed and ascribed to a field-induced biaxiality, i.e., the deformation of the helical structure due to a coupling between the dielectric anisotropy and the electric field. The temperature dependence of the nonlinear spectrum was also discussed. [S1063-651X(96)11306-4]

PACS number(s): 64.70.Md, 77.22.Gm, 77.84.−s

I. INTRODUCTION

Antiferroelectric liquid crystals (AFLC) [1] have attracted the attention of many researchers not only for their potential to an alternative type display application but also for the fundamental interest in their structures and phase transitions since the discovery of tristable switching in 4-(1-methyl-heptyloxycarbonylphenyl) 4′-octylbiphenyl-4-carboxylate (MHPOBC) in the chiral smectic-C_A (Sm-C_A^*) phase [2] and the herring bone molecular alignment in 1-methyl-heptyl-terephthalidene-bis-aminocinnamate (MHTAC) in the smectic-O^* phase [3]. These smectic liquid crystals often show a variety of new electroactive smectic-*C* phases such as the ferrielectric Sm-C_γ^* phase [4], the antiferroelectric Sm-C_A^* phase, and the mysterious Sm-C_α^* phase [5] besides the conventional ferroelectric Sm-C^* phase. In the Sm-C_A^* phase, the constituent molecules tilt from the layer normal with their tilt directions almost opposite in the adjacent layers [3,6,7] (herring bone structure) and form a helical structure due to their chirality [6,8]. In this antiferroelectric structure, the spontaneous polarization vectors in the adjacent layers point to almost antiparallel directions and are canceled macroscopically even in the helix unwound state.

As the dielectric response of AFLCs is sensitive to their phase transitions and structures, the dielectric measurement has become one of the popular tools for designating the phase sequences and investigating the phase transitions of AFLCs [9,10]. In the Sm-C_A^* phase, at least three relaxation modes are observed by the dielectric measurement [11–13]. These modes are distinguished from each other by the temperature dependence of their relaxation times and are assigned to the following three modes, respectively: the ferroelectric soft mode, the molecular rotation around its short axis, and the field induced Goldstone mode under a dc bias electric field. The Goldstone mode is dielectric inactive in the Sm-C_A^* phase where the spontaneous polarization is canceled locally and thus it is not observable in the linear dielectric relaxation spectroscopy without a dc bias electric field [12–14]. This mode is only detectable directly by the quasielastic light scattering (photon correlation) method [15,16].

Recently, the dielectric relaxation spectroscopy has been extended to the nonlinear regime and applied to a variety of materials including ferroelectric polymers [17,18] and ferroelectric liquid crystals [19,20]. In these materials, the nonlinear dielectric relaxation is regarded as a higher-order effect on the motional mode of molecular dipoles in the materials due to the applied electric field and has its counterpart in the linear relaxation spectrum. The nonlinear dielectric spectrum is expected to give more detailed information on the molecular motion and the microscopic environment of dipoles compared with the linear one.

In this paper we have applied the nonlinear dielectric measurement to an AFLC in the vicinity of the Sm-*A*–Sm-C_A^* phase transition and in the Sm-C_A^* phase. The frequency spectrum of the third-order nonlinear dielectric constant ε_3 in the Sm-C_A^* phase is found to be a Debye-type one which has no counterpart in the linear spectrum. This nonlinear spectrum is theoretically explained by the deformation of the helical structure induced by the electric field through the dielectric anisotropy in AFLCs.

II. EXPERIMENT

Under the weak applied electric field E, the electric displacement D can be expanded as the power series of E as $D=\sum_{n=1}^{\infty}\varepsilon_n E^n$. When the applied field is a sinusoidal one with the amplitude E_0 and the angular frequency ω much lower than the relaxation angular frequency, D is expressed as a sum of the fundamental and higher-order harmonic components D_n $(n=1,2,\ldots,)$ as [17,21]

$$D_n=\sum_{r=0}^{\infty} {}_{m+2r}C_r\,\varepsilon_{m+2r}\left(\frac{E_0}{2}\right)^{m+2r}. \qquad (1)$$

We can obtain the nth-order nonlinear dielectric constant ε_n by fitting the measured D_n to Eq. (1) taking into account the lowest-order terms with $r=0$ and 1.

The applied electric field was generated from the synthesizer HP3325A (Hewlett-Packard) in the frequency range from 20 Hz to 300 kHz. The electric displacement D detected by the charge amplifier was digitized and averaged on the storage oscilloscope DL3100 (Yokogawa) with a 12-bit resolution. The AFLC used in this study is (R)-4-(1-trifluoromethyl-heptyloxycarbonyl) phenyl 4′-octyloxybiphenyl-4-carboxylate (TFMHPOBC) which has a chemical structure similar to MHPOBC, but a phase sequence (Isotropic-Sm-A–Sm-C_A^*-Crystal) simpler than other AFLCs [22]. The AFLC sample was sandwiched between two glass plates with indium-tin-oxide (ITO) electrodes separated by a film spacer. The sample surfaces were spin coated with polyimide and rubbed unidirectionally to attain a homogeneous alignment of liquid crystals. The cell gap was about 20 μm which was determined by measuring the capacitance of an empty cell.

III. RESULTS AND DISCUSSION

The temperature dependences of the linear and third-order nonlinear dielectric constants ε_1, ε_3 at 5 kHz in the Sm-A and the Sm-C_A^* phases are shown in Figs. 1(a) and 1(b), respectively. Here, ε_0 is the vacuum permittivity. The linear constant ε_1 clearly shows a critical behavior near the Sm-A–Sm-C_A^* phase transition temperature. This is due to the softening of the ferroelectric soft mode, which arises from the fluctuation of directors in the tilt angle direction. The critical behavior of ε_1 in the Sm-C_A^* phase is not so sharp compared with those reported by other authors [11,13] and thus this transition is not to be clearly assigned to the first-order one. As the temperature decreases below the transition temperature, ε_1 approaches to a constant value nearly equal to ε_1 in the Sm-A phase at the higher temperature.

The third-order nonlinear dielectric constant ε_3 is positive both in the Sm-A and Sm-C_A^* phases. In the Sm-A phase, the temperature dependence of ε_3 shows a critical behavior in a similar way to ε_1. The critical behaviors of ε_1 and ε_3 in this phase can be analyzed by the Landau-type phenomenological theory [23] with only a ferroelectric order parameter [24] even for the Sm-A–Sm-C_A^* phase transition. In previous papers [21], we studied theoretically the critical behaviors of ε_1 and ε_3 in the Sm-A phase near the Sm-A–Sm-C^* phase transition and the agreement with experiment was satisfactory. It is found in the present study that ε_1 consists of two terms: a temperature-independent term and a term exhibiting a critical temperature dependence with an exponent of unity (conventional Curie-Weiss–type behavior) due to a coupling between the tilt angle and the polarization. The third-order constant ε_3 also shows a critical behavior with an exponent of four and its sign is dependent on the order of the phase transition, i.e., $\varepsilon_3<0$ for the second-order transition and $\varepsilon_3>0$ for the first-order one [21]. The best-fitted theoretical curves with a critical exponent of one for ε_1 and that of four for ε_3 are shown as solid lines in Figs. 1(a) and 1(b), respectively. The linear relationship between ε_1 and $\varepsilon_3^{1/4}$ [21] is also confirmed in Fig. 1(c). The good agreement between experiment and theory implies the applicability of the Landau-type phenomenological theory to the critical behavior in the Sm-A phase near the Sm-A–Sm-C_A^* phase transition. The positive sign of ε_3 in the Sm-A phase indicates that the ferroelectric order parameter of TFMHPOBC shows the first-order transition. It has been actually reported that the Sm-C^* phase appears between the Sm-A and Sm-C_A^* phases in the racemized sample of TFMHPOBC and the Sm-A–Sm-C^* phase transition is the first-order one [14].

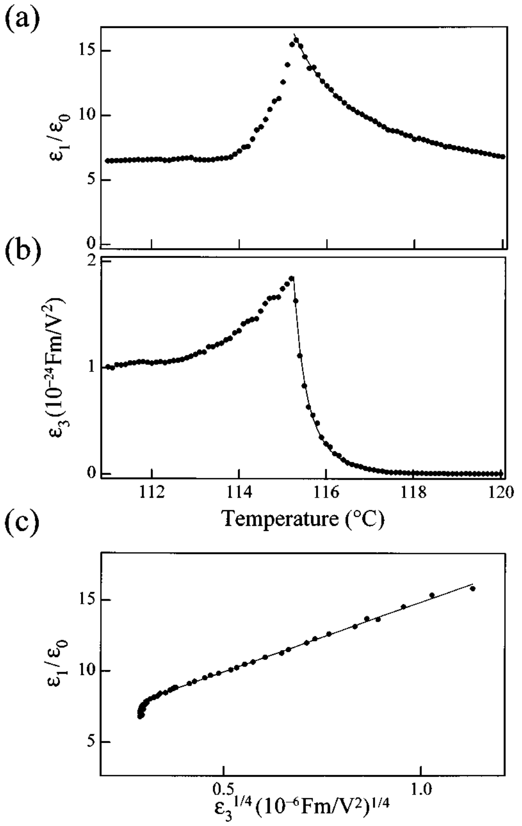

FIG. 1. The temperature dependences of (a) the linear dielectric constant ε_1 and (b) the third-order nonlinear dielectric constant ε_3 at 5 kHz in the Sm-A and Sm-C_A^* phases of (R)-TFMHPOBC. (c) The relation between ε_3 and the linear dielectric constant ε_1 in the Sm-A phase.

The contribution of the ferroelectric soft mode to ε_3 in the Sm-C_A^* phase should decrease sharply on cooling in accordance with the temperature dependence of ε_1. The remaining positive large value of ε_3 in the Sm-C_A^* phase is not explainable by the contribution of the soft mode. Instead, we can consider the deformation of the helical structure due to the applied electric field as an origin of the dielectric nonlinearity in the Sm-C_A^* phase. In this case, there are two possible mechanisms for the induced polarization: one is the reorientation of spontaneous polarization not fully cancelled and the other is the change of dielectric constant due to the deformation. In the former case, the nonlinear dielectric spectra would exhibit a Debye-type relaxation extended to the higher order and with a negative sign [19,20]. However, the sign of ε_3 experimentally obtained is positive and the profile of the observed spectrum also differs from the theoretically calculated one as is shown later. We will then discuss the latter case, i.e., the change of bulk dielectric constant due to the deformation of helix under the electric field in the following.

The main contribution to the dielectric response in the Sm-C_A^* phase is a coupling between the dielectric tensor $\overleftrightarrow{\varepsilon}$ and the applied electric field E, because the macroscopic spontaneous polarization disappears in this phase due to the orientation of constituent molecules. The local dielectric tensor is obtained by rotating twice the tensor with the principle values ε_1, ε_2, and ε_3, starting from the local frame which first coincides with the laboratory frame (x,y,z). The tensor is rotated by the tilt angle θ around the y axis and further rotated by the azimuthal angle ϕ around the z axis. The local dielectric tensor in the Sm-C_A^* phase can be replaced by the tensor averaged in the successive two layers with the same tilt angle θ and the azimuthal angles approximately given by ϕ and $\phi+\pi$, respectively. We can finally obtain the macroscopic (bulk) dielectric tensor in the Sm-C_A^* phase by spatially averaging the two-layer local tensor over one helical pitch l as [25]

$$\overleftrightarrow{\varepsilon}=\begin{pmatrix} \frac{1}{2}\{(\varepsilon_1+\varepsilon_2)+(\varepsilon_3-\varepsilon_1)\sin^2\theta\} & 0 & 0 \\ 0 & \frac{1}{2}\{(\varepsilon_1+\varepsilon_2)+(\varepsilon_3-\varepsilon_1)\sin^2\theta\} & 0 \\ 0 & 0 & \varepsilon_1\sin^2\theta+\varepsilon_3\cos^2\theta \end{pmatrix}$$

$$+\frac{1}{2}\{(\varepsilon_1-\varepsilon_2)+(\varepsilon_3-\varepsilon_1)\sin^2\theta\}\begin{pmatrix} \langle\cos 2\phi\rangle & \langle\sin 2\phi\rangle & 0 \\ \langle\sin 2\phi\rangle & -\langle\cos 2\phi\rangle & 0 \\ 0 & 0 & 0 \end{pmatrix}, \tag{2}$$

where $\langle\rangle$ denotes a spatial average taken along the layer normal direction (the z axis) over one helical pitch. When the electric field is absent, the average values $\langle\cos 2\phi\rangle$ and $\langle\sin 2\phi\rangle$ vanish and the dielectric tensor given by Eq. (2) becomes uniaxial. When the electric field is applied, the spatial distribution of the helical structure is deformed by the coupling between the dielectric anisotropy $\Delta\varepsilon$ $[\equiv(\varepsilon_1-\varepsilon_2)+(\varepsilon_3-\varepsilon_1)\sin^2\theta]$ and the electric field in a quite similar way to the cholesteric liquid crystal under the electric field [26].

The spatial distribution of the azimuthal angle ϕ along the z axis under the ac electric field $E=E_0\cos\omega t$ with the amplitude E_0 and the angular frequency ω can be expressed by the following torque balance equation derived from the free energy density with the electric field applied parallel to the y axis:

$$K\frac{\partial^2\phi}{\partial z^2}-\gamma\frac{\partial\phi}{\partial t}+\frac{1}{2}\,\Delta\varepsilon E^2\sin 2\phi=0, \tag{3}$$

where K is the effective elastic constant and γ is the rotational viscosity. The solution of Eq. (3) under a weak electric field is obtained as a perturbational form up to the order E_0^2 with reference to the field-free state $\phi=q_0z=2\pi z/l$ as

$$\phi=q_0z+\sum_{r=0}^{2}A_{22r}\left(\frac{E_0}{2}\right)^2e^{i(2-2r)\omega t}\sin(2q_0z), \tag{4}$$

where

$$A_{220}=A_{222}^*=\frac{\Delta\varepsilon}{8Kq_0^2(1+i\omega\tau)},\quad A_{221}=\frac{\Delta\varepsilon}{4Kq_0^2},\quad \tau=\frac{\gamma}{2Kq_0^2}.$$

From solution (4), the average values $\langle\cos 2\phi\rangle$ and $\langle\sin 2\phi\rangle$ are calculated as

$$\langle\cos 2\phi\rangle=-\sum_{r=0}^{2}A_{22r}\left(\frac{E_0}{2}\right)^2e^{i(2-2r)\omega t}, \tag{5}$$

$$\langle\sin 2\phi\rangle=0. \tag{6}$$

The dielectric tensor in the Sm-C_A^* phase under the electric field is written as a biaxial form with no off-diagonal elements. The y component of induced polarization, P, is calculated from Eqs. (2) and (5) and the relation $P=\int_0^{E_0}\varepsilon_{yy}(E)dE$ with $dE=dE_0\cos\omega t$. The linear, second-, and third-order nonlinear dielectric constants, ε_n^* ($n=1$, 2, and 3), are calculated from the definition $\varepsilon_n^*=\lim_{E_0\to0}[(P_{nn}^*)/(E_0^n)]2^{n-1}$ as

$$\varepsilon_1=\tfrac{1}{2}\{(\varepsilon_1+\varepsilon_2)+(\varepsilon_3-\varepsilon_1)\sin^2\theta\}, \tag{7}$$

$$\varepsilon_2=0, \tag{8}$$

$$\varepsilon_3^*=\frac{(\Delta\varepsilon)^2}{48Kq_0^2}\,\frac{1}{1+i\omega\tau}\equiv\frac{\Delta\varepsilon_3}{1+i\omega\tau_3}, \tag{9}$$

where P_{11}^*, P_{22}^*, and P_{33}^* are the complex amplitudes of the fundamental, the second-order, and the third-order harmonic components of the electric displacement, which are proportional to E_0, E_0^2, and E_0^3, respectively.

The linear dielectric constant ε_1 has no frequency dispersion and is written as a combination of three principle values of dielectric tensor and the tilt angle. The second-order non-

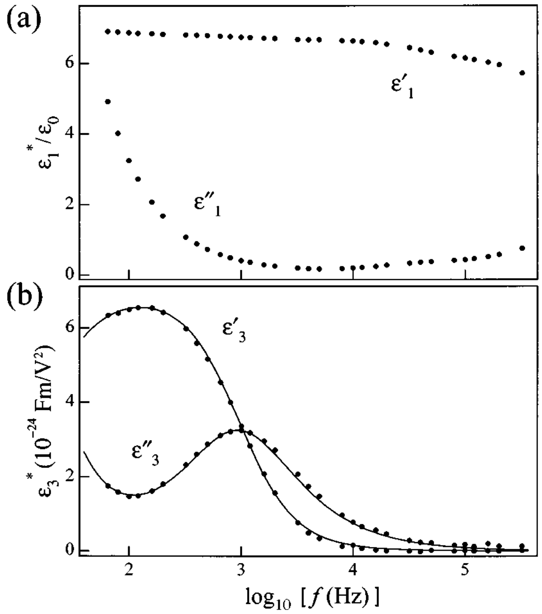

FIG. 2. (a) The frequency dependences of the linear dielectric constant ε_1^* and (b) the third-order nonlinear dielectric constant ε_3^* in the Sm-C_A^* phase of (R)-TFMHPOBC at 85 °C.

linear dielectric constant ε_2 vanishes due to the symmetry. The third-order nonlinear constant ε_3^* shows a single relaxation of Debye type which reflects the fluctuation of the helical structure and its relaxation time τ_3 is identified with that of the (antiferroelectric) Goldstone mode in the Sm-C_A^* phase. The sign of the increment $\Delta\varepsilon_3$ is positive in contrast to the negative sign of $\Delta\varepsilon_3$ in the Sm-C^* phase and in agreement with the observed sign of $\Delta\varepsilon_3$. In the case of the Sm-C^* phase, ε_3^* arises mainly from the saturation of the spontaneous polarization due to the electric field and its magnitude is much larger than that in the Sm-C_A^* phase. The nonlinear spectrum ε_3^* due to spontaneous polarization shows an extended form of Debye-type relaxation as shown in previous studies [19]. To confirm the theoretical prediction, we experimentally investigated the frequency spectra of ε_1^* $(=\varepsilon'_1 - i\varepsilon''_1)$ and ε_3^* $(=\varepsilon'_3 - i\varepsilon''_3)$ in the Sm-C_A^* phase at 85 °C. The results are shown in Figs. 2(a) and 2(b), respectively. It is found that the linear constant ε_1^* takes almost a constant value except in the low frequency region where the electrode polarization and the sample conductivity are dominant, and there are two small relaxations at about 100 kHz and above 1 MHz. In contrast, the nonlinear constant ε_3^* clearly shows a single relaxation of Debye-type around 1 kHz, but no relaxation in ε_1^* is observed corresponding to this nonlinear relaxation spectrum. The obtained spectrum of ε_3^* can be fitted to the Debye-type relaxation with the parameter β_3 expressing the distribution of relaxation times as

$$\varepsilon_3^*(\omega) = \frac{\Delta\varepsilon_3}{1+(i\omega\tau_3)^{\beta_3}} + \frac{\sigma_3}{(i\omega)^{\gamma_3}}, \tag{10}$$

where $\Delta\varepsilon_3$, τ_3, and σ_3 are the third-order nonlinear dielectric increment, the relaxation time, and the apparent nonlinear conductivity with the adjustable parameter γ_3. The solid line in Fig. 2(b) is the best-fitted curve of Eq. (10) to the measured spectrum. We can conclude that the main origin of ε_3^* in the Sm-C_A^* phase is the field-induced biaxiality due to the deformation of helical structure through the coupling between the dielectric anisotropy and the electric field.

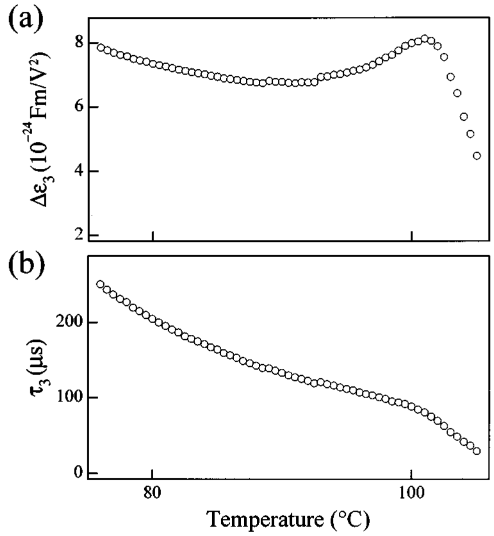

FIG. 3. The temperature dependences of (a) the increment $\Delta\varepsilon_3$ and (b) the relaxation time τ_3 of the third-order nonlinear dielectric constant ε_3^* in the Sm-C_A^* phase of (R)-TFMHPOBC.

The temperature dependences of $\Delta\varepsilon_3$ and τ_3 are plotted in Figs. 3(a) and 3(b), respectively. The parameter β_3 is about 0.95 except in the vicinity of the transition temperature and thus the relaxation can be regarded as almost a single one. The temperature dependence of $\Delta\varepsilon_3$ is quite similar to that of the linear spectrum for the Goldstone mode in the Sm-C^* phase [19]. The obtained value of $\Delta\varepsilon_3$ is much smaller than in the case of the ferroelectric liquid crystals [19,20] where $\Delta\varepsilon_3$ is proportional to the fourth power of the spontaneous polarization. However, $\Delta\varepsilon_3$ in the Sm-C_A^* phase is still large compared to those for ferroelectric or polar polymers [17,18]. By assuming, as the material parameters, the likely values $K_3 = 1\times10^{-12}N$, $\theta = 10°$, $l = 1$ μm, and $\Delta\varepsilon/\varepsilon_0 = 2$, we have a rough estimation of $\Delta\varepsilon_3$ as 5.3 $\times10^{-24}$ Fm/V^2, which is in agreement with the experimentally obtained value in the order of magnitude. The value of τ_3 increases monotonously in a sub ms range and is almost the same order as the relaxation time of the Goldstone mode in the Sm-C^* phase. The relaxation frequency of the Goldstone mode of MHPOBC in the Sm-C_A^* phase measured by the photon-correlation method was a few hundred kHz [15,16], much higher than that obtained in the present study. It is also reported that the nonlinear electro-optic response shows the Debye-type relaxation in the Sm-C_A^* phase of MHPOBC with a relaxation frequency different from the photon-correlation measurement [12]. This discrepancy may be ascribed partly to the differences in the sample alignment, but the reason is still obscure at present.

IV. CONCLUSION

We have applied the nonlinear dielectric relaxation spectroscopy to the Sm-A and Sm-C_A^* phases of the antiferroelectric liquid crystal TFMHPOBC. In the Sm-A phase, the critical behaviors of ε_1 and ε_3 are observed and well explained by the phenomenological theory of Landau type. In the Sm-C_A^* phase, we can detect by measuring ε_3^* the Goldstone mode which is not to be observed by the linear dielectric spectroscopy without a dc bias electric field. In other words, the nonlinear relaxation in the present case is different from those studied before in that it has no counterparts in the linear spectrum. Though the linear and nonlinear relaxations which arise directly from the fluctuation of helical structure are forbidden by a structure symmetry in the Sm-C_A^* phase, this fluctuation can be indirectly detected in the nonlinear response through the deformation of helical structure due to the electric field. This type of nonlinear response shows a further possibility of the nonlinear dielectric relaxation spectroscopy.

ACKNOWLEDGMENT

This work was partly supported by a Grant-in-Aid for Scientific Research from the Ministry of Education, Science, Sports and Culture.

[1] A. Fukuda, Y. Takanishi, T. Isozaki, K. Ishikawa, and H. Takezoe, J. Mater. Chem. **4**, 997 (1994).
[2] A. D. L. Chandani, T. Hagiwara, Y. Suzuki, Y. Ouchi, H. Takezoe, and A. Fukuda, Jpn. J. Appl. Phys. **27**, L729 (1988).
[3] Y. Galerne and L. Liebert, Phys. Rev. Lett. **66**, 2891 (1991).
[4] E. Gorecka, A. D. L. Chandani, Y. Ouchi, H. Takezoe, and A. Fukuda, Jpn. J. Appl. Phys. **29**, 131 (1990).
[5] K. Hiraoka, Y. Takanishi, K. Skarp, H. Takezoe, and A. Fukuda, Jpn. J. Appl. Phys. **30**, L1819 (1991).
[6] A. D. L. Chandani, E. Gorecka, Y. Ouchi, H. Takezoe, and A. Fukuda, Jpn. J. Appl. Phys. **28**, L1265 (1989).
[7] Ch. Bahr and D. Fliegner, Phys. Rev. Lett. **70**, 1842 (1993).
[8] Ji Li, H. Takezoe, and A. Fukuda, Jpn. J. Appl. Phys. **30**, 532 (1991).
[9] K. Hiraoka, A. D. L. Chandani, E. Gorecka, Y. Ouchi, H. Takezoe, and A. Fukuda, Jpn. J. Appl. Phys. **29**, L1473 (1990).
[10] H. Takezoe, K. Hiraoka, T. Isozaki, K. Miyachi, H. Aoki, and A. Fukuda, in *Modern Topics in Liquid Crystals*, edited by A. Buka (World Scientific, Singapore, 1993), p. 319.
[11] H. Orihara, T. Fujikawa, Y. Ishibashi, Y. Yamada, N. Yamamoto, K. Mori, K. Nakamura, Y. Suzuki, T. Hagiwara, and I. Kawamura, Jpn. J. Appl. Phys. **29**, L333 (1990).
[12] K. Hiraoka, H. Takezoe, and A. Fukuda, Ferroelectrics **147**, 13 (1993).
[13] H. Moritake, M. Ozaki, and K. Yoshino, Jpn. J. Appl. Phys. **32**, L1432 (1993).
[14] T. Fujikawa, H. Orihara, Y. Ishibashi, Y. Yamada, N. Yamamoto, K. Mori, K. Nakamura, Y. Suzuki, T. Hagiwara, and I. Kawamura, Jpn. J. Appl. Phys. **30**, 2826 (1991).
[15] H. Sun, H. Orihara, and Y. Ishibashi, J. Phys. Soc. Jpn. **60**, 4175 (1991); **62**, 2066 (1993).
[16] I. Muševič, B. Žekš, R. Blinc, M. Čopič, M. M. Wittebrood, Th. Rasing, H. Orihara, and Y. Ishibashi, Phys. Rev. Lett. **71**, 1180 (1993).
[17] T. Furukawa, K. Nakajima, T. Koizumi, and M. Date, Jpn. J. Appl. Phys. **26**, 1039 (1987).
[18] T. Furukawa, M. Tada, K. Nakajima, and Y. Seo, Jpn. J. Appl. Phys. **27**, 200 (1988).
[19] Y. Kimura and R. Hayakawa, Jpn. J. Appl. Phys. **32**, 4571 (1993).
[20] H. Orihara, A. Fukase, and Y. Ishibashi, J. Phys. Soc. Jpn. **64**, 976 (1995).
[21] Y. Kimura and R. Hayakawa, Mol. Cryst. Liq. Cryst. **261**, 225 (1995).
[22] Y. Yamada, K. Mori, N. Yamamoto, H. Hayashi, K. Nakamura, M. Yamawaki, H. Orihara, and Y. Ishibashi, Jpn. J. Appl. Phys. **28**, L1606 (1989).
[23] H. Orihara and Y. Ishibashi, Jpn. J. Appl. Phys. **29**, L115 (1990).
[24] S. A. Pikin and V. L. Indenbom, Usp. Fiz. Nauk. **125**, 251 (1978) [Sov. Phys. Usp. **21**, 487 (1978)].
[25] I. Muševič, B. Žekč, and R. Blinc, Phys. Rev. E **47**, 1094 (1993).
[26] P. G. de Gennes and J. Prost, *Physics of Liquid Crystals* (Plenum, New York, 1992), 2nd ed.